Phosphoregulation of Nap1 Plays a Role in Septin Ring Dynamics and Morphogenesis in *Candida albicans*

Zhen-Xing Huang,[a] Pan Zhao,[a] Gui-Sheng Zeng,[a] Yan-Ming Wang,[a] Ian Sudbery,[b] Yue Wang[a,c]

Institute of Molecular and Cell Biology, Agency for Science, Technology and Research, Singapore[a]; Department of Physiology, Anatomy and Genetics, University of Oxford, Oxford, United Kingdom[b]; Department of Biochemistry, Yong Loo Lin School of Medicine, National University of Singapore, Singapore[c]

ABSTRACT **Nap1 has long been identified as a potential septin regulator in yeasts. However, its function and regulation remain poorly defined. Here, we report functional characterization of Nap1 in the human-pathogenic fungus *Candida albicans*. We find that deletion of *NAP1* causes constitutive filamentous growth and changes of septin dynamics. We present evidence that Nap1's cellular localization and function are regulated by phosphorylation. Phos-tag gel electrophoresis revealed that Nap1 phosphorylation is cell cycle dependent, exhibiting the lowest level around the time of bud emergence. Mass spectrometry identified 10 phosphoserine and phosphothreonine residues in a cluster near the N terminus, and mutation of these residues affected Nap1's localization to the septin ring and cellular function. Nap1 phosphorylation involves two septin ring-associated kinases, Cla4 and Gin4, and its dephosphorylation occurs at the septin ring in a manner dependent on the phosphatases PP2A and Cdc14. Furthermore, the *nap1*Δ/Δ mutant and alleles carrying mutations of the phosphorylation sites exhibited greatly reduced virulence in a mouse model of systemic candidiasis. Together, our findings not only provide new mechanistic insights into Nap1's function and regulation but also suggest the potential to target Nap1 in future therapeutic design.**

IMPORTANCE **Septins are conserved filament-forming GTPases involved in a wide range of cellular events, such as cytokinesis, exocytosis, and morphogenesis. In *Candida albicans*, the most prevalent human fungal pathogen, septin functions are indispensable for its virulence. However, the molecular mechanisms by which septin structures are regulated are poorly understood. In this study, we deleted *NAP1*, a gene encoding a putative septin regulator, in *C. albicans* and found that cells lacking *NAP1* showed abnormalities in morphology, invasive growth, and septin ring dynamics. We identified a conserved N-terminal phosphorylation cluster on Nap1 and demonstrated that phosphorylation at these sites regulates Nap1 localization and function. Importantly, deletion of *NAP1* or mutation in the N-terminal phosphorylation cluster strongly reduced the virulence of *C. albicans* in a mouse model of systemic infection. Thus, this study not only provides mechanistic insights into septin regulation but also suggests Nap1 as a potential antifungal target.**

Received 10 December 2013 **Accepted** 26 December 2013 **Published** 4 February 2014

Citation Huang Z-X, Zhao P, Zeng G-S, Wang Y-M, Sudbery I, Wang Y. 2014. Phosphoregulation of Nap1 plays a role in septin ring dynamics and morphogenesis in *Candida albicans*. mBio 5(1):e00915-13. doi:10.1128/mBio.00915-13.

Editor Judith Berman, University of Minnesota, GCD

Address correspondence to Yue Wang, mcbwangy@imcb.a-star.edu.sg.

Septins are filament-forming proteins first discovered in the budding yeast *Saccharomyces cerevisiae* for their roles in cytokinesis (1). Subsequently, they have been implicated in diverse cellular events in eukaryotes (2–4). All species studied so far contain two or more septin isoforms. Septin molecules form linear oligomers, which in turn assemble into higher-order structures at cellular sites associated with specific functions (5). Like actin cables and microtubules, septin structures are assembled and disassembled in highly controlled manners. An example is the assembly and disassembly of the septin ring at the bud neck of yeast cells at the start and the end of a cell cycle, respectively (6, 7). The septin ring serves as a scaffold that recruits cell cycle regulatory proteins, including checkpoint regulators (8–10), as well as a membrane diffusion barrier between the bud and mother compartments (11, 12). In the pathogenic fungus *Candida albicans*, septins localize to the tip of hyphae and play a role in recruiting polarity proteins (13).

The molecular mechanisms dictating when and how a septin structure is assembled or disassembled remain unclear. In *S. cerevisiae*, ~100 proteins interact with the septin ring (14, 15). However, only a few have been shown to play a role in regulating septin organization and dynamics, such as the Rho GTPase Cdc42; several septin-associated protein kinases, Cla4, Elm1, and Gin4; and a nucleosome assembly protein, Nap1 (6, 16). Currently, how these proteins are organized into signaling pathways remains controversial. Tjandra et al. (17) proposed that Gin4 acts downstream of Nap1 and Cla4, while another study suggested that Nap1 and Cla4 regulate the septins through Gin4-independent pathways (6). Despite these uncertainties, studies in both *S. cerevisiae* and *C. albicans* identified a strong association of Nap1 and Gin4 with the septins (18, 19), suggesting that they might be key septin regulators. Recent studies in *C. albicans* revealed that Gin4 phosphorylates the septin Cdc11, priming it for further phosphorylation by the cyclin-dependent kinase (Cdk) Cdc28 during hyphal growth

(20). Furthermore, depleting Gin4 in G_1 cells blocks septin ring formation (19). However, how Nap1 regulates the septins remains largely unknown.

Nap1 was first found in mammalian cells for its role in nucleosome assembly (21), and more recently, its homologues have been linked to a range of seemingly unrelated functions (22), including cell cycle progression (18, 23), transcription regulation (24), and septin organization (6, 16). The *S. cerevisiae* Nap1 was first found as a binding partner of the cyclin Clb2 and for its role in mitosis (23). In yeast cells, Nap1 localizes primarily to the bud neck. However, it was seen in the nucleus when a nuclear export signal (NES) was deleted (25). A structural study revealed that the NES is masked by a domain harboring several target sites for casein kinase 2 (CK2) (26). Later, phosphomapping by mass spectrometry (MS) detected phosphorylation at 11 serine/threonine residues, three of which were confirmed to be CK2 substrate (27) and important for Nap1's nuclear localization. However, how Nap1 regulates the septin ring and the role of phosphorylation at the rest of the phosphorylated residues remain undetermined.

C. albicans is a major human fungal pathogen causing life-threatening infections (28). This pathogen is able to switch between the yeast and hyphal forms of growth (29). The hyphal growth facilitates tissue penetration, and yeast cells are required for dissemination through the circulation system. Several lines of evidence indicate that septins play a crucial role in hyphal growth and virulence. First, upon hyphal induction, septins first localize to a small cortical area from which the germ tube emerges and later localize to the tip of germ tubes and hyphae (30). Second, deleting a septin gene, *CDC10* or *CDC11*, resulted in hyphal defects, poor tissue penetration, and reduced virulence (7, 31). Third, Hgc1/Cdc28, a key hyphal promoter (32), phosphorylates Cdc11 (20). Thus, understanding septin organization and function in *C. albicans* will not only shed light on mechanisms of septin regulation but can also reveal new therapeutic targets.

In this study, we have characterized *nap1*Δ/Δ mutants in *C. albicans* and studied Nap1 phosphorylation and its roles in regulating its cellular localization, interaction with septins, and cell morphogenesis. We have also evaluated the role of Nap1 in the virulence of *C. albicans*.

RESULTS

Deletion of *C. albicans NAP1* causes constitutive filamentous growth. We previously reported that Gin4 and Cdks regulate hyphal growth through phosphoregulation of the septins in *C. albicans* (19, 20). To further unravel the underlying molecular mechanisms, we continue to study proteins that have been implicated in the regulation of Gin4 and Cdks. Previous findings of Nap1's association with Clb2 and Gin4 in *S. cerevisiae* (18, 23) prompted us to investigate its *C. albicans* homologue. Using the *S. cerevisiae* Nap1 (ScNap1) sequence to search the *C. albicans* protein database, we found a 49% identity with an uncharacterized protein encoded by orf19.7501, which was thus named *C. albicans* Nap1 (CaNap1). To determine its function, we first constructed *nap1*Δ/Δ mutants. We noted that unlike wild-type (WT) cells that grew colonies with a smooth surface, the *nap1*Δ/Δ cells formed wrinkled colonies with filaments emanating from the edge (Fig. 1A), indicating filamentous growth. *nap1*Δ/Δ cells also invaded the agar. The colonies could not be washed off the agar surface as easily as could WT cells (Fig. 1B), and microscopic examination of the agar sections underneath the mutant colonies revealed deep penetration by fungal filaments (Fig. 1C). Consistently, in liquid cultures, many *nap1*Δ/Δ cells exhibited elongation and swelling at 30°C (Fig. 1A). This phenotype was enhanced at 37°C with the formation of many pseudohyphae, whereas WT cells grew as yeast cells under the same conditions (Fig. 1A). However, true hyphal growth was unaffected in *nap1*Δ/Δ cells under all conditions tested (data not shown). Reintegrating a WT copy of *NAP1* at its native locus in the *nap1*Δ/Δ mutant fully rescued the defects (Fig. 1).

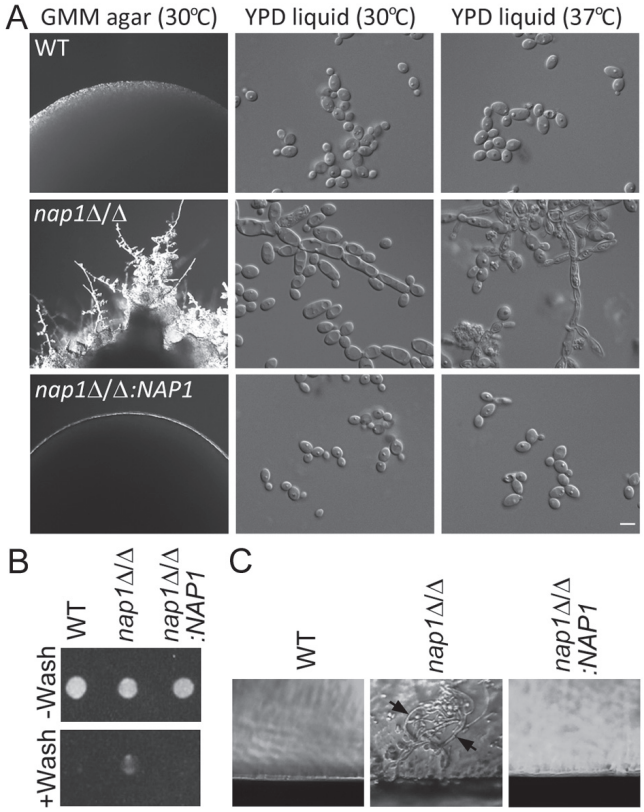

FIG 1 *nap1*Δ/Δ cells exhibit constitutive filamentous and invasive growth. (A) WT (BWP17; all strains used in this study are listed in Table S1 in the supplemental material) (47), *nap1*Δ/Δ (HZX01), and *NAP1*-reintegrated (HZX02) cells were grown on GMM plates and incubated at 30°C for 5 days and in liquid YPD at 30°C or 37°C overnight. Size bars, 5 μm throughout the figures. (B) Cells were spotted onto GMM plates and incubated at 30°C for 5 days. The spots were photographed before and after washing the plate with water. (C) Agar sections underneath the colonies were examined and photographed under a microscope. Arrows indicate fungal filaments.

Nap1 colocalizes with septins, and its localization requires proper septin organization. CaNap1 was previously identified in affinity-purified septin complexes (19), suggesting colocalization with the septins. To determine if and when Nap1 colocalizes with the septins, we constructed a strain expressing a functional Nap1-green fluorescent protein (GFP) fusion as the sole source of this protein under the control of its native promoter. In yeast cells, Nap1-GFP first localized at the presumptive budding site and then at the tip of the emerging bud. When the small bud was taking shape, Nap1-GFP formed a ring at the bud neck, which persisted until cytokinesis when the ring split into two parallel rings (Fig. 2A). During hyphal growth, Nap1-GFP localized first to the tip of the germ tubes and later formed a band marking the site of

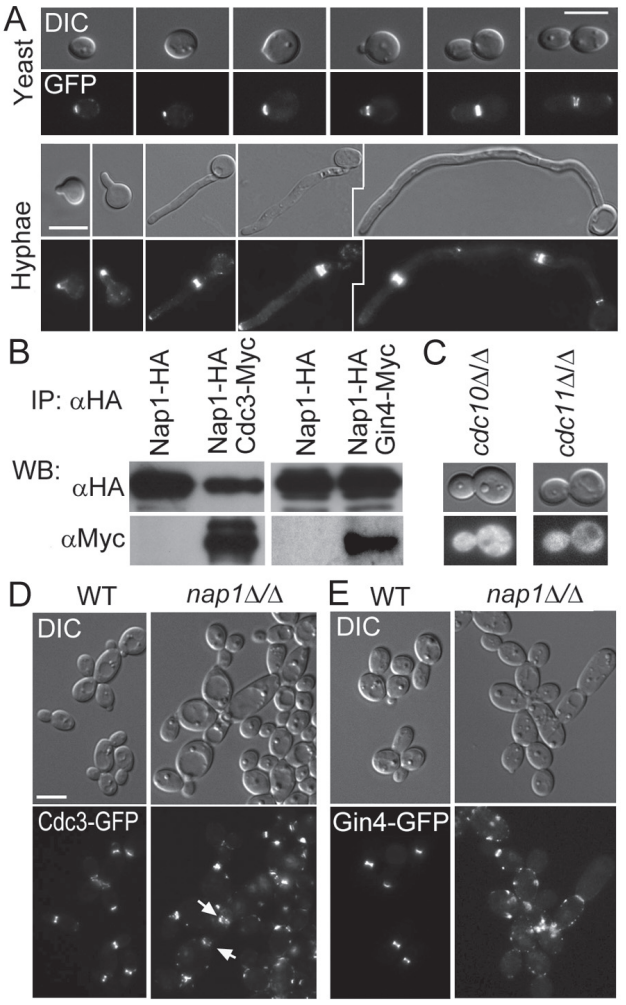

FIG 2 Nap1 subcellular localization and its interaction with septins. (A) An overnight culture of cells expressing Nap1-GFP (HZX02) was grown in GMM at 30°C for yeast cells or in GMM plus 20% serum at 37°C for hyphal induction before differential interference contrast (DIC) and fluorescence microscopy. Cells at different stages of growth are shown. (B) Co-IP of Cdc3 and Gin4 with Nap1. Cell extracts were prepared from log-phase yeast cells of HZX05 (*NAP1-HA CDC3-Myc*) and HZX06 (*NAP1-HA GIN4-Myc*) and subjected to IP using HA antibody (αHA), followed by WB with αHA and αMyc. HZX03 (*NAP1-HA*) was included as a negative control. (C) Mislocalization of Nap1-GFP in septin mutants. Yeast cells of HZX18 (*cdc10*Δ/Δ *NAP1-GFP*) and HZX19 (*cdc11*Δ/Δ NAP1-GFP) were imaged as described for panel A. (D) Septin localization and organization defects in *nap1*Δ/Δ cells. Log-phase yeast cells of HZX27 (WT; *CDC3-GFP*) and HZX26 (*nap1*Δ/Δ *CDC3-GFP*) were examined for morphology and Cdc3-GFP localization. Arrows show septin defects. (E) Gin4 localization and organization defects in *nap1*Δ/Δ cells. Log-phase yeast cells of HZX48 (WT; *GIN4-GFP*) and HZX47 (*nap1*Δ/Δ *GIN4-GFP*) were examined for morphology and Gin4-GFP localization.

the septum, and the band split into two bands at cytokinesis which did not disassemble, at least through the next cell cycle (Fig. 2A). The dynamic localization of Nap1 closely resembles that of the septins (33, 34). Consistently, Western blot (WB) analysis showed that hemagglutinin (HA)-tagged Nap1 coimmunoprecipitated (co-IP) with Myc-tagged Cdc3 and Gin4 (Fig. 2B).

The septin ring recruits proteins to the bud neck (14, 35). To ask if Nap1's cellular localization depends on the septins, Nap1-GFP was expressed in the *cdc10*Δ/Δ and *cdc11*Δ/Δ mutants, in which the septin ring can form but with abnormalities (7). Interestingly, we found Nap1-GFP entirely in the cytoplasm in both mutants (Fig. 2C). WB analysis showed that the cellular levels of Nap1-GFP in the septin mutants were comparable to that in WT cells (see Fig. S1 in the supplemental material). Thus, the data indicate that proper septin ring organization is required for recruiting Nap1 to the bud neck.

We also examined if Nap1 is required for septin ring assembly by expressing Cdc3-GFP in the *nap1*Δ/Δ mutant. We found that although septin rings formed at the bud neck in most yeast cells with a normal morphology, abnormalities in both septin localization and organization were often observed in the elongated cells (Fig. 2D): the septin rings frequently appeared broken, and random dots were present in many cells as well. The defects were stronger at 37°C than at 30°C, consistent with the presence of more pseudohyphae at 37°C. Previously, we reported that the septin ring assembly depends on the kinase-independent functions of Gin4 (19). It is thus possible that Gin4's localization to the bud neck and its function were also impaired in the *nap1*Δ/Δ mutant. Consistent with this idea, Gin4-GFP in the *nap1*Δ/Δ cells also mislocalized in ways similar to Cdc3-GFP (Fig. 2E), suggesting that the abnormalities in Gin4 localization might be responsible for the septin defects in the *nap1*Δ/Δ mutant. However, it is also possible that Nap1 has both direct and indirect roles in regulating septin ring assembly.

N-terminal phosphorylation is crucial for Nap1 localization and function. Cell cycle-dependent phosphorylation plays a key role in regulating the structure and function of the septins and their associated proteins (19, 20). To ask if Nap1 is also phosphoregulated, we performed Phos-tag gel electrophoresis (36) and WB analysis of protein extracts and detected Nap1 as two bands. The slower-migrating one disappeared after pretreatment of the sample with λ-phosphatase (λPP), indicating a phosphoisoform (Fig. 3A). We next examined if Nap1 phosphorylation is cell cycle dependent. We used centrifugal elutriation to collect early G_1 cells, >95% of which had not formed the new septin ring, and then released them into glucose minimal medium (GMM) for growth at 30°C. Aliquots of cells were collected at timed intervals to determine the budding index as well as the phosphorylation status of Nap1. Phosphorylation at each time point was quantified by measuring the band intensity and calculating the intensity ratio of phosphorylated to unphosphorylated Nap1 (Phos/Unphos). Figure 3B shows that the Phos/Unphos ratio was at the highest (~1.0) in newly collected G_1 cells, declined when the cells were traversing through the G_1 phase, and reached the lowest level of ~0.51 around the time of bud emergence. The Phos/Unphos ratio increased and remained high through the rest of the cell cycle until the beginning of the next one, when it decreased again. The data demonstrated that Nap1 phosphorylation is cell cycle dependent. To map the phosphorylation sites, Nap1-GFP was isolated from yeast cells using GFP-Trap for MS analysis. Twelve phosphorylated serine (S) and threonine (T) residues were detected. Interestingly, 10 of the 12 residues resided from S16 to T52 near the N terminus. Phosphorylation at similar sites was also observed in ScNap1 (27), suggesting that the phosphorylation has a conserved but yet undefined function. The other two phosphoresidues are S403 and S411, which are not conserved in ScNap1.

We next studied the physiological significance of Nap1 phosphorylation in the N-terminal region. All 10 phosphorylated residues, S16, T20, T24, S27, T29, S31, S35, T42, S46, and T52, were

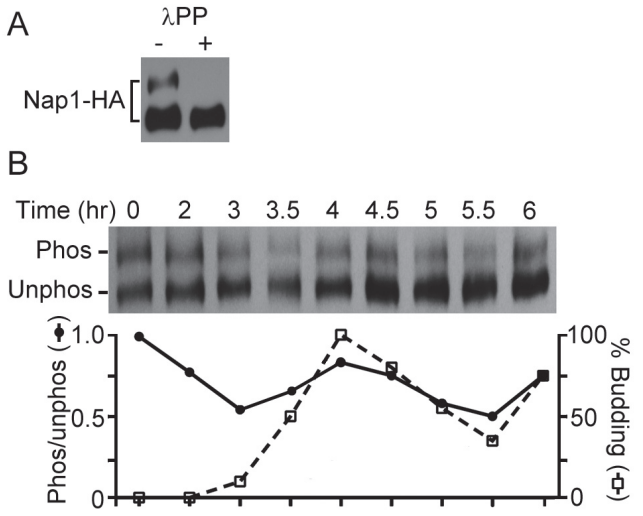

FIG 3 Cell cycle-dependent phosphorylation of Nap1. (A) Log-phase yeast cells expressing Nap1-HA (HZX03) were subjected to IP with αHA. The IP product was divided into two halves, and one was treated with λPP. Nap1 phosphorylation was analyzed using Phos-tag SDS-PAGE followed by αHA WB. (B) G_1 cells of HZX03 were released into YPD at 30°C for growth. Aliquots were harvested at intervals to derive a budding index and for Phos-tag analysis. The intensity of Nap1 bands was quantified using ImageJ, and the Phos/Unphos ratio of Nap1 at each time point was calculated.

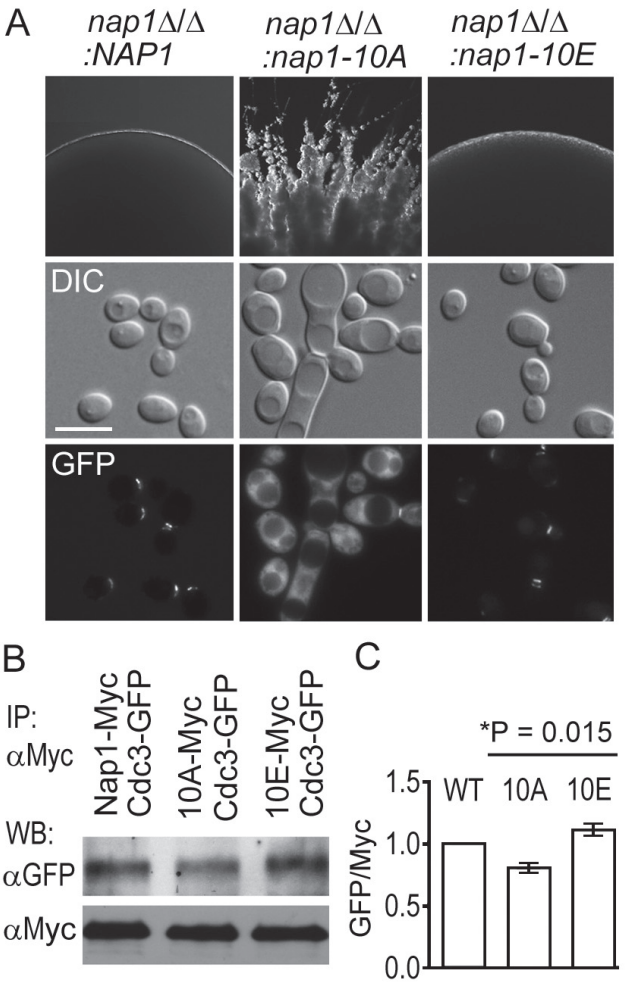

FIG 4 Phosphorylation of Nap1 is crucial for its localization and function. (A) WT Nap1 (HZX02), Nap1-10A (HZX07), or Nap1-10E (HZX08) was expressed as a GFP fusion protein in *nap1*Δ/Δ cells. Colony morphology on GMM plates (top) and cell morphology in liquid YPD at 30°C (middle) were examined. Nap1 localization was visualized by fluorescence microscopy (bottom). (B) Co-IP of Cdc3 with WT Nap1, Nap1-10A, or Nap1-10E. Cell extracts were prepared from log-phase yeast cells of HZX15 (*NAP1-Myc CDC3-GFP*), HZX13 (*nap1-10A-Myc CDC3-GFP*), and HZX14 (*nap1-10E-Myc CDC3-GFP*). Nap1 was immunoprecipitated with αMyc. Nap1 and Cdc3 in the IP products were detected with αMyc and αGFP WB, respectively. (C) The intensity of protein bands shown in panel B was determined by using ImageJ, and the ratio of Cdc3 to Nap1 in each lane was calculated. Student's *t* test was performed. Error bars represent standard errors.

mutated to either the nonphosphorylatable alanine (*nap1-10A*) or the phosphomimetic glutamic acid (*nap1-10E*). To evaluate the function of Nap1-10A and Nap1-10E, they were tagged at the C terminus with GFP, HA, or Myc and expressed in the *nap1*Δ/Δ mutant from the native promoter. We first examined the abilities of the two alleles to rescue the growth defects of the *nap1*Δ/Δ mutant. We found that while *nap1-10E* could largely rescue the defects, *nap1-10A* failed to do so (Fig. 4A), indicating that the N-terminal phosphorylation of Nap1 is important for yeast morphogenesis. Next, we examined the cellular localization of Nap1-10A-GFP and Nap1-10E-GFP. Strikingly, Nap1-10A was found primarily in the cytoplasm with only a faint signal at the bud neck, whereas Nap1-10E localized normally to the bud neck (Fig. 4A). The observation suggested that Nap1 phosphorylation is important for its bud neck localization. We thought that the mislocalization of Nap1-10A might reflect weakened interaction with the septins. In support of this idea, repeated co-IP experiments consistently showed an ~20% decrease in the interaction between Nap1-10A and Cdc3 and an ~11% increase between Nap1-10E and Cdc3 compared with that between WT Nap1 and Cdc3 (Fig. 4B and C). The co-IP experiments were performed on cells grown at both 30°C and 37°C, which produced similar results, and WB analysis showed that the cellular levels of both mutant Nap1 proteins were comparable to that of the WT protein (data not shown). The moderate changes detected by co-IP in the interaction between Nap1-10A and Cdc3 are apparently in contrast to the strong reduction of Nap1-10A localization at the bud neck. A plausible explanation is that the mutations might have mainly affected Nap1's interaction with the septin polymers at the bud neck without significantly reducing its affinity for the septin molecules in the cytoplasm. Taken together, the data suggest that phosphorylation in the N terminus has a role in regulating Nap1's localization to the bud neck.

Nap1 dephosphorylation depends on its bud neck localization. We next examined the phosphorylation status of Nap1-10A and Nap1-10E. Unexpectedly, both proteins exhibited a Phos/Unphos ratio greater than 2 (Fig. 5A). This was in contrast to the WT Nap1, which had a Phos/Unphos ratio of <1.0. This may suggest that mutating the 10 phosphorylation sites led to enhanced phosphorylation at other sites, which might occur only transiently in WT cells and/or at sites which are normally not phosphorylated. It is also possible that the mutations may influence Nap1 dephosphorylation due to mislocalization of the protein or change of the structural context required for dephosphorylation. To begin to test these hypotheses, we examined if Nap1 phosphorylation depends on its localization to the bud neck. To

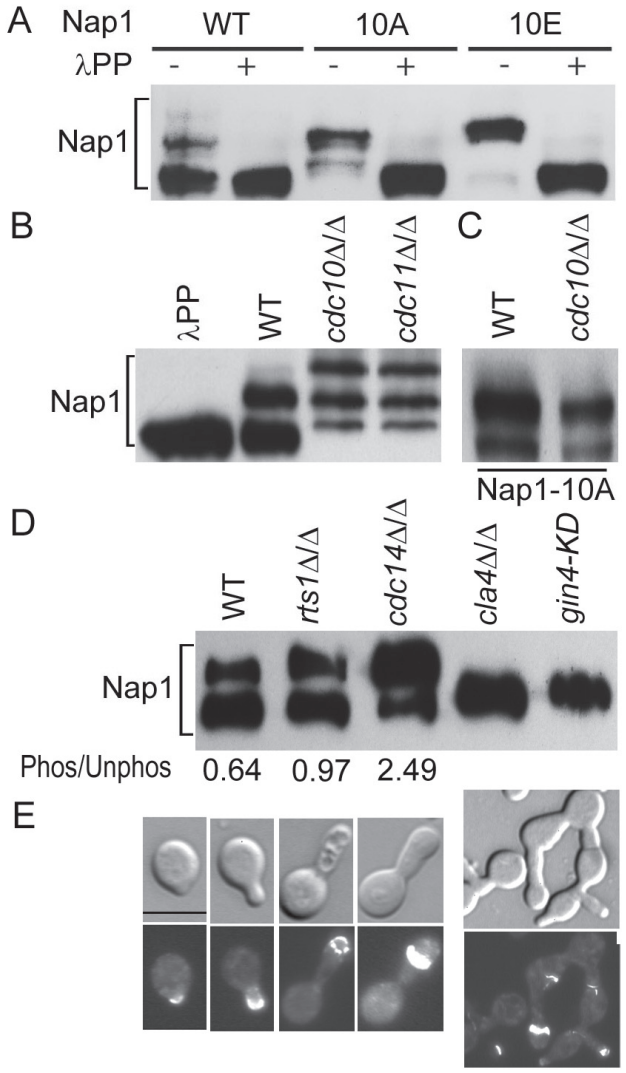

FIG 5 Phos-tag WB analysis of WT Nap1, Nap1-10A, and Nap1-10E. (A) Nap1-HA (HZX03), Nap1-10A-HA (HZX09), and Nap1-10E-HA (HZX10) were immunoprecipitated from log-phase yeast cells with αHA. Half of each IP product was treated with λPP before Phos-tag gel electrophoresis and αHA WB. (B) Phos-tag WB analysis of Nap1-HA in WT (HZX03), *cdc10*Δ/Δ (HZX20), and *cdc11*Δ/Δ (HZX21) cells. Experiments were done as described for panel A. (C) Phos-tag WB comparison of Nap1-10A in WT and *cdc10*Δ/Δ cells. Experiments were done as described for panel A using log-phase yeast cells of HZX09 (*nap1-10A*-HA) and HZX22 (*nap1-10A*-HA *cdc10*Δ/Δ). (D) Phos-tag WB analysis of Nap1 phosphorylation in kinase and phosphatase mutants. Experiments were done as described for panel A using log-phase yeast cells of HZX03 (*NAP1-HA*), HZX41 (*NAP1-HA rts1*Δ/Δ), HZX42 (*NAP1-HA cdc14*Δ/Δ), HZX43 (*NAP1-HA cla4*Δ/Δ), and HZX44 (NAP1-HA *gin4-KD*). (E) Septin localization in *cla4*Δ/Δ yeast cells. G_1 yeast cells of HZX45 (*cla4*Δ/Δ *CDC3-GFP*) were released into GMM for growth at 30°C, and cells at different stages of growth were examined for morphology and septin localization.

this end, we analyzed Nap1 phosphorylation in *cdc10*Δ/Δ and *cdc11*Δ/Δ mutants in which Nap1 localized to the cytoplasm (Fig. 2C). Strikingly, Nap1 in both mutants showed not only large amounts of phosphoisoforms but also an additional band with much lower mobility compared with Nap1 in WT cells (Fig. 5B). The data strongly suggest that the regulation of Nap1 phosphorylation requires its localization to the bud neck. We next examined the phosphorylation status of Nap1-10A and Nap1-10E in *cdc10*Δ/Δ cells. Surprisingly, although Nap1-10A in *cdc10*Δ/Δ cells showed a high Phos/Unphos ratio, as it did in WT cells, it did not show the slowest-migrating phosphoisoform observed for WT Nap1 in the same septin mutants (Fig. 5C). This lack of further phosphorylation of Nap1-10A in *cdc10*Δ/Δ cells suggested that the phosphorylation sites in Nap1-10A might overlap the additional phosphorylation sites in WT Nap1 when expressed in the septin mutant. This is consistent with the fact that both Nap1-10A in WT cells and WT Nap1 in the septin mutants fail to localize to the bud neck. We were unable to detect Nap1-10E in the *nap1*Δ/Δ *cdc10*Δ/Δ and *nap1*Δ/Δ *cdc11*Δ/Δ mutants (see Fig. S2 in the supplemental material), although it was expressed in exactly the same way as Nap1-10A, indicating that Nap1-10E is highly unstable in the septin mutants.

The coincidence of greater Nap1 phosphorylation with its failure to localize to the bud neck suggested that Nap1 might be dephosphorylated at the bud neck in WT cells. Next, we examined Nap1 phosphorylation in *rts1*Δ/Δ and *cdc14*Δ/Δ mutants. Rts1 is a regulatory subunit of protein phosphatase 2A (PP2A), and Cdc14 is a phosphatase that regulates the mitotic exit. Both phosphatases transiently localize to the bud neck (37, 38). In this experiment, WT, *rts1*Δ/Δ, and *cdc14*Δ/Δ cells with tagged Nap1 were grown to the log phase. Phos-tag gel analysis revealed a significant increase in the Phos/Unphos ratio of Nap1 in both mutants, 0.97 in *rts1*Δ/Δ and 2.49 in *cdc14*Δ/Δ cells, in comparison with 0.64 in WT cells (Fig. 5D). Thus, the data support the idea that Nap1 is dephosphorylated on the septin ring and is dependent on Cdc14 and Rts1.

We next asked if the septin-associated kinases Cla4 and Gin4 are involved in Nap1 phosphorylation. We used a *cla4*Δ/Δ mutant and a *gin4-KD* (kinase-dead) mutant (19). While the role of Gin4 in septin organization is well established (19, 20, 39), the effect of *CLA4* deletion on the septins had not been reported in *C. albicans*. Thus, we first examined septin behavior in *cla4*Δ/Δ cells. Figure 5E shows that although Cdc3-GFP localized to the presumptive budding site, it failed to form a septin ring at the bud neck. Instead, the septins remained at the bud tip, leading to an elongated bud. Only at a later stage was a septin ring formed close to the tip. *cla4*Δ/Δ cells were also defective in cytokinesis/cell separation, forming clusters of cells with mislocalized septins. The results confirmed a role for Cla4 in regulating the septin ring. Next, we examined Nap1 phosphorylation in *cla4*Δ/Δ and *gin4-KD* mutants. Strikingly, we found that Nap1 phosphorylation was abolished in both mutants (Fig. 5D), showing dependence of Nap1 phosphorylation on Cla4 and Gin4.

Genetic interaction of *NAP1* and *CDC10*. To gain more insight into the functional relationship between Nap1 and septins, we investigated the genetic interaction between *nap1*Δ/Δ and *cdc10*Δ/Δ mutants. We compared the morphological phenotypes of the single mutants and the double mutant. Although the morphology of *cdc10*Δ/Δ yeast cells was rather normal, deletion of *CDC10* together with *NAP1* caused a much stronger filamentous phenotype than did deleting *NAP1* alone (Fig. 6A). The pseudohyphal phenotype of the *nap1*Δ/Δ *cdc10*Δ/Δ mutant was corrected when a WT copy of *NAP1* was introduced. The results demonstrated a genetic interaction between *NAP1* and *CDC10*, indicating that they contribute to the same cellular process at least par-

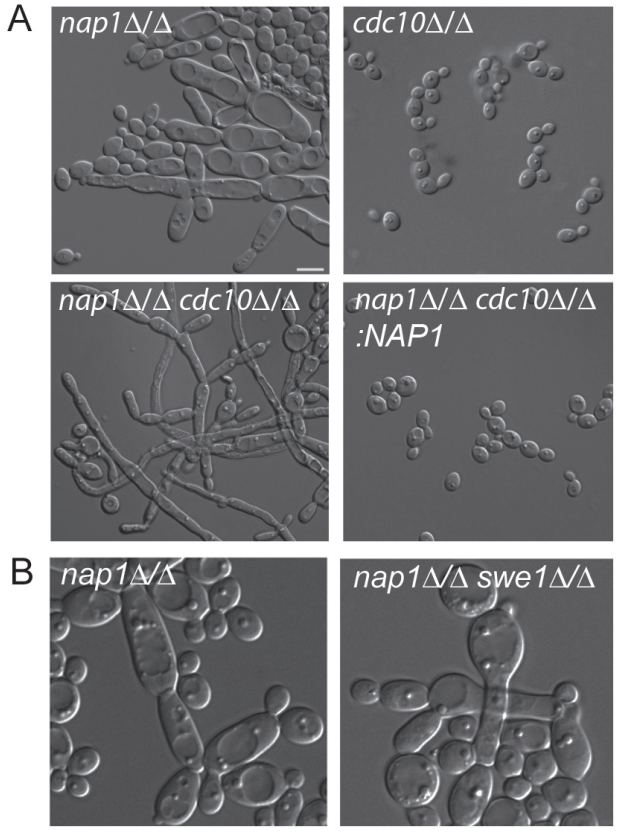

FIG 6 Genetic interaction between *nap1*Δ/Δ and *cdc10*Δ/Δ mutants and independence of *nap1*Δ/Δ pseudohyphal growth on Swe1. (A and B) Cells of the indicated genotypes were grown overnight in liquid YPD at 30°C before imaging.

tially through parallel pathways or work in the same protein complex.

The pseudohyphal growth of *nap1*Δ/Δ cells does not depend on Swe1. In *S. cerevisiae*, septin defects often result in filamentous growth through a Swe1-mediated morphogenesis checkpoint (40). In *C. albicans*, the *hsl1*Δ/Δ mutant undergoes Swe1-mediated pseudohyphal growth (41). To determine if Swe1 has a role in the filamentous growth in the *nap1*Δ/Δ mutant, we constructed a *nap1*Δ/Δ *swe1*Δ/Δ mutant and found that deleting *SWE1* had no significant effect (Fig. 6B), suggesting that the filamentous growth of *nap1*Δ/Δ is independent of Swe1. Wightman et al. (39) also reported a weak dependence of pseudohyphal growth on Swe1 in the *gin4*Δ/Δ mutant.

Deletion of *NAP1* affects septin ring stability. Septin ring dynamics plays an important role in cell division and morphogenesis (37, 42). Next, we conducted fluorescence recovery after photobleaching (FRAP) analysis to determine if the deletion of *NAP1* affects septin ring dynamics. To visualize the septin ring, we tagged Cdc3 with GFP. FRAP analysis was performed at three different budding stages, namely, in small-budded cells, large-budded cells with a single ring, and large-budded cells with split rings. The full ring was bleached, and fluorescence recovery was recorded at 1-min intervals (see Fig. S3 in the supplemental material). In WT cells, the fluorescence intensity of Cdc3-GFP recovered to a maximum of ~60% in small-budded cells and ~40% in large-budded cells with either a single ring or split rings (Fig. 7). Interestingly, in *nap1*Δ/Δ cells, the recovery was consistently higher in all three budding stages, suggesting that the septin rings assembled in the absence of Nap1 are more dynamic.

To determine if the change of septin dynamics in the *NAP1* mutants affects the timing of septin ring disassembly, we used time-lapse imaging to record the time elapsed between the time of septin ring split and that of ring disappearance at the end of the cell cycle in WT, *nap1-10A*, and *nap1-10E* cells. However, we did not detect a significant difference between the WT and the mutant cells (data not shown). A possible explanation is that the moderate changes in septin ring dynamics observed in the *NAP1* mutants are not sufficient to cause a significant shift in the timing of septin disassembly. Alternatively, septin ring disassembly and dynamics may not always be coupled.

***NAP1* mutants have decreased virulence.** Next, we asked if Nap1 is important for the virulence of *C. albicans*. We first determined the growth rates of the mutants in GMM at 37°C. We found that the doubling times of the *NAP1* mutants were not significantly different from that of the WT (Fig. 8A). To test virulence, we conducted intravenous infections of BALB/c mice. To assess the abilities of the mutants to colonize the kidney, we counted CFU per kidney 2 days postinoculation (Fig. 8B, top). The mice infected with the WT strain had ~3.3 × 10^5 CFU/kidney. In sharp

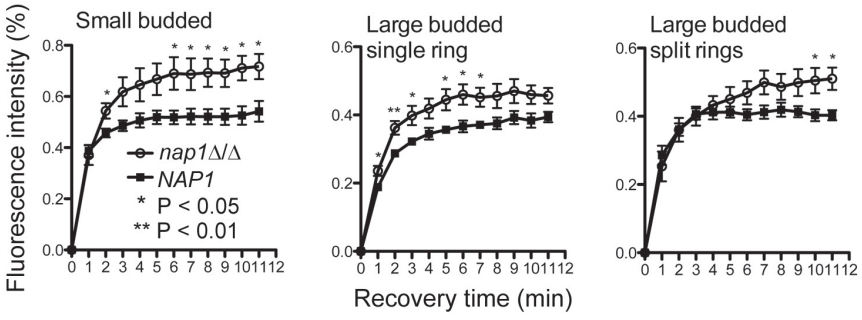

FIG 7 Septin ring dynamics in *nap1*Δ/Δ cells. FRAP analysis of Cdc3-GFP in the septin ring in WT (HZX27) and *nap1*Δ/Δ (HZX26) yeast cells with a small bud, a large bud with a single ring, and a large bud with split rings (cell images are shown in Fig. S3 in the supplemental material). Fluorescence intensity was measured at 1-min intervals after photobleaching of the septin ring. Average values taken from 5 cells of each budding stage were used to generate the curves. Student's *t* tests were performed, and error bars represent standard errors.

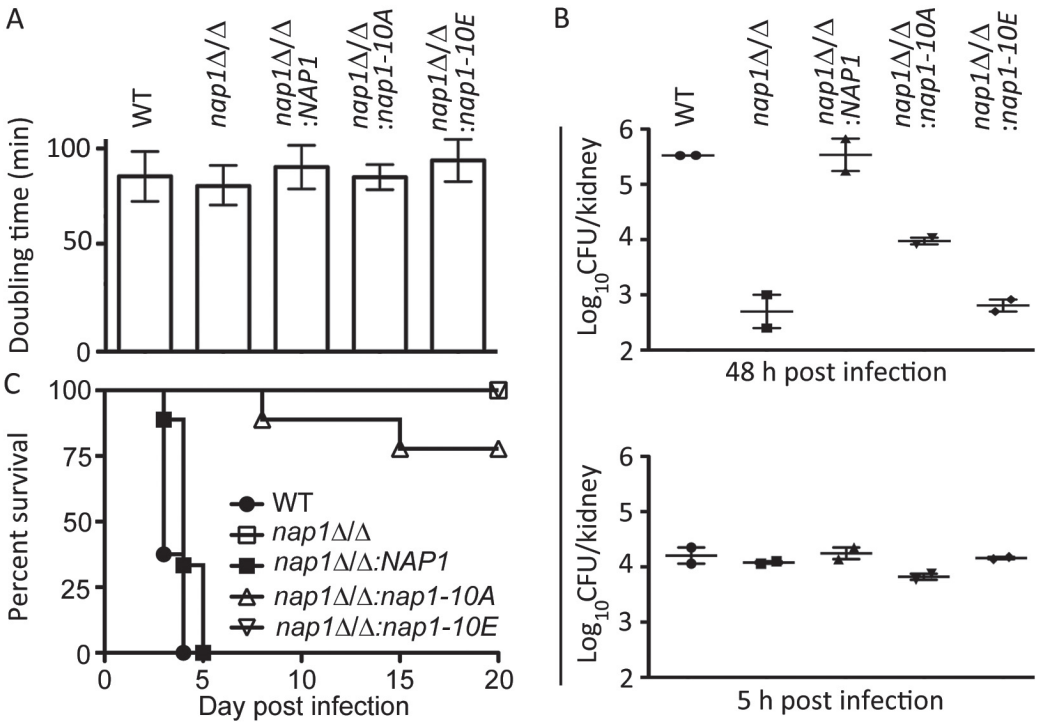

FIG 8 *NAP1* mutants exhibited reduced virulence. (A) Doubling times of strains. Cells were grown in YPD at 37°C, and optical density at 600 nm was measured at regular intervals. Doubling times were calculated by averaging optical density values measured during the log phase of growth from 3 independent experiments. Error bars represent 1 standard deviation from the mean. (B) CFU/kidney of infected mice. Two mice for each *C. albicans* strain were sacrificed 48 h or 5 h postinfection to determine CFU/kidney. (C) Survival curve of mice ($n = 8$ per strain) injected with 1×10^6 cells with the indicated genotype.

contrast, the CFU/kidney from the animals infected with the *nap1*Δ/Δ mutant was ~1,000 times less (6.1×10^2). The reintegrant strain produced 4.2×10^5 CFU/kidney, comparable to the WT strain. Interestingly, despite the fact that Nap1-10E, but not Nap1-10A, can significantly alleviate the growth defects of the *nap1*Δ/Δ mutant, both *nap1-10A* and *nap1-10E* mutants showed poor colonization of the kidney, as they produced 8.3×10^3 and 6.6×10^2 CFU/kidney, respectively. All mice infected with the WT or the reintegrant strain died within 5 days. Among the mice infected with the mutants, only two mice infected with the *nap1-10A* mutant died later, on the 8th and 15th days (Fig. 8C). As the *nap1*Δ/Δ mutant forms pseudohyphae at 37°C, we thought that the filamentous shape might prevent the cells from reaching the kidney effectively. To test this idea, we sacrificed mice 5 h after inoculation to count the CFU/kidney but found no significant difference between mice infected with the WT strain and those infected with the *nap1*Δ/Δ mutants (Fig. 8B, bottom). The results indicate that the attenuation of virulence in the *NAP1* mutants is not a consequence of pseudohyphal growth. Most likely, the capacity for proliferation or survival of the mutants in the host is compromised. Nevertheless, the tests demonstrate that Nap1 is crucially required for the virulence of *C. albicans*.

Comparison of transcriptomes between WT and *nap1*Δ/Δ cells. In *S. cerevisiae*, Nap1 has been implicated in the regulation of gene expression. However, we do not observe CaNap1 localizing to the nucleus even after deleting a putative NES, deletion of which in ScNap1 causes a nuclear localization (27). Furthermore, the CK2 phosphorylation sites required for nuclear localization in ScNap1 (26) are not conserved in CaNap1. To confirm that deletion of *NAP1* acts primarily through effects on the septin ring rather than through gene regulation, we performed microarray analysis comparing gene expression in WT cells to that in *nap1*Δ/Δ mutants. In total, 142 genes changed in expression by at least 2-fold at a 5% false discovery rate (FDR) threshold, 53 up and 89 down (see Table S2 in the supplemental material). KEGG and GO enrichment analysis revealed that many of these genes were related to the metabolism of glucose (KEGG pathways such as "glycolysis/gluconeogenesis" and "carbon metabolism" and GO terms such as "carbohydrate metabolic process" were identified); in particular, genes in the glycolytic pathway were downregulated (see Table S3).

DISCUSSION

Phosphoregulation of Nap1 in *C. albicans*. In this study, we found that CaNap1 is phosphorylated in a cell cycle dependent manner and identified a cluster of phospho-S/T residues near the N terminus. Unlike WT Nap1 that localized to the bud neck, the nonphosphorylatable mutant Nap1-10A localized mainly in the cytoplasm. Also, the Nap1-10A mutant failed to rescue the morphological defects of *nap1*Δ/Δ cells. In contrast, the phosphomimetic Nap1-10E exhibited normal localization and could significantly correct the morphological defects of the *nap1*Δ/Δ mutant. Therefore, the N-terminal phosphorylation of Nap1 is important for its function. Our data further suggest that the phosphorylation may regulate Nap1's interaction with the septins, because co-IP experiments detected reduced interaction of Nap1-10A and in-

creased interaction of Nap1-10E with Cdc3. However, the high instability of Nap1-10E observed in the *nap1*Δ/Δ *cdc10*Δ/Δ background and its negative impact on virulence in mice clearly indicate that Nap1-10E is not fully functional.

Other than the phosphorylation at the 10 N-terminal sites identified by MS, it is likely that Nap1 is also phosphorylated at other sites that MS failed to detect, as both Nap1-10A and Nap1-10E showed a significantly higher phosphorylation level than the WT protein. As Nap1-10A localized primarily to the cytoplasm, we hypothesized that some residues of Nap1 may be phosphorylated in the cytoplasm and then dephosphorylated once Nap1 localizes to the septin ring. This hypothesis is supported by the observation of Nap1 hyperphosphorylation in the *cdc10*Δ/Δ and *cdc11*Δ/Δ mutants where Nap1 also fails to localize to the septin ring. Furthermore, the fact that Nap1-10A did not show a further increase in its phosphorylation level when expressed in the septin mutants suggests that the additional phosphorylation caused by the 10A mutation is likely to have occurred at the same residues as that caused by the deletion of *CDC10* or *CDC11*. Although the exact mechanism of Nap1 dephosphorylation remains unclear, we discovered that two septin-associated protein phosphatases, PP2A and Cdc14, are involved in this process. We realize that the above argument is unable to explain the hyperphosphorylation of Nap1-10E, which apparently can localize to the septin ring. One possible explanation is that the phosphomimetic mutations caused phosphorylation at sites that are poor substrates of phosphatases or the phosphorylation caused structural changes that render the sites inaccessible to phosphatases. The extreme instability of Nap1-10E observed in *nap1*Δ/Δ *cdc10*Δ/Δ cells is in agreement with this explanation.

Calvert et al. (27) reported that Nap1 is phosphoregulated in *S. cerevisiae*. They identified about a dozen phosphoresidues on Nap1 and demonstrated that 3 residues near the C terminus are targets of CK2. Notably, the rest of the phosphorylated residues were found in a cluster near the N terminus, although the role of phosphorylation was not determined. Not all the phosphorylated residues found in ScNap1 are conserved in CaNap1. For example, the three CK2 sites are not found in CaNap1 by sequence alignment. As these CK2 sites are important for the nuclear localization of Nap1 in *S. cerevisiae* (27), their absence may imply that Nap1 has reduced nuclear function in *C. albicans*. Consistently, we have never detected Nap1 in the nucleus in *C. albicans*, even when we disrupted the putative NES (data not shown), mutation of which in ScNap1 caused Nap1 nuclear localization (27). We found that Nap1 phosphorylation was completely abolished in *cla4*Δ/Δ and *gin4-KD* mutants, suggesting that the two septin-associated kinases play an important role in the regulation of Nap1 phosphorylation. The role could be direct or indirect or both, and future investigation is required to distinguish these possibilities. As Nap1, Cla4, and Gin4 also regulate septin organization in *S. cerevisiae* (6, 17), the phosphoregulation of Nap1 elucidated in this study may have revealed evolutionarily conserved mechanisms for septin regulation in fungi. The septin and morphological defects observed in the *NAP1* mutants together with the dependence of its phosphorylation on septin-associated kinases and phosphatases strongly support the idea that Nap1's role in *C. albicans* is primarily at the bud neck, but not through the regulation of gene expression. This view is supported by the microarray data.

Attenuated virulence of *NAP1* mutants. The *nap1*Δ/Δ and the *nap1-10A* and *nap1-10E* mutants exhibited greatly reduced virulence in the mouse model of candidemia. All mice infected with the *nap1*Δ/Δ or *nap-10E* mutant and 75% of the mice infected with the *nap1-10A* mutant survived to the end of the experiment, whereas all those infected with the WT or the *NAP1* reintegrant strain died within 5 days. Warenda et al. (31) reported that both *cdc10*Δ/Δ and *cdc11*Δ/Δ mutants are defective in virulence. As these septin mutants also destabilize the septin ring (7), the impaired virulence of the *NAP1* mutants could also be a result of septin ring defects. When looked at closely, however, there are distinct features in the defects between *NAP1* and septin mutants. The *nap1*Δ/Δ and *nap1-10A* cells showed enhanced invasive growth on agar, whereas septin mutants are defective in invasive growth. The septin mutants showed normal colonization of the kidney, and the reduced virulence was likely due to their defects in tissue invasion. As the average CFU/kidney of mice infected with *nap1*Δ/Δ and *nap1-10A* cells at day 2 was ~1,000-fold less than that for the WT strain, we thought that the pseudohyphal growth of the mutant cells might have reduced their ability to travel through the blood vessels to reach the kidney for colonization. Consistent with this view, Umeyama et al. (41) demonstrated that *hsl1*Δ/Δ mutant cells, which also exhibit filamentous growth and invasion of agar, have reduced virulence due to defective organ colonization. However, when we sacrificed the mice at 5 h postinfection, we did not observe a significant difference in CFU/kidney between mice infected with the WT strain and those infected with the *nap1*Δ/Δ mutant. Thus, the attenuated virulence of the *NAP1* mutants in mice may be a result of impairment of other abilities required for pathogenesis, such as the ability to survive and proliferate in the host. A surprising result was the loss of virulence in the *nap1-10E* mutant, which seemed indistinguishable from WT cells in growth and morphology. However, the extreme instability of Nap1-10E in the *nap1*Δ/Δ *cdc10*Δ/Δ mutant indicates that Nap1-10E is not fully functional, which could underlie the loss of virulence. Regardless of the exact mechanisms by which Nap1 contributes to infection, the critical dependence of *C. albicans* virulence on Nap1 in mouse suggests that new antifungal drugs may be developed by targeting Nap1.

MATERIALS AND METHODS

Medium preparation, phosphorylation site mapping, protein extraction, immunoprecipitation, Western blotting, and microscopy. Medium preparation, phosphorylation site mapping, protein extraction, immunoprecipitation, Western blotting, and microscopy were performed as described previously (13, 20).

Gene deletion and reintegration. Strain BWP17 (43) was used to create all the gene deletion mutants in this study. A gene deletion cassette contained a selection marker gene, *URA3*, *HIS1*, or *ARG4*, flanked with DNA fragments corresponding to the 5′ and 3′ untranslated region of the gene. The two copies of *NAP1* were deleted with the recyclable *hisG-URA3-hisG* cassette, so that all three selection markers (*HIS1*, *ARG4*, and *URA3*) can be used for subsequent genetic manipulations. All gene deletion mutants were verified by PCR. To reintegrate the WT or mutated *NAP1* gene into the *nap1*Δ/Δ mutant, the full-length *NAP1* open reading frame (ORF) together with the 971-bp upstream promoter region sequence was PCR amplified with KpnI and XhoI sites added to the 5′ and 3′ ends, respectively. The amplified DNA fragment was cloned in frame with a C-terminal Myc, HA, or GFP tag in the *CIP10* vector (44). A PmeI site was generated in the promoter region for linearization by site-directed mutagenesis using the QuikChange multi-site-directed mutagenesis kit (Agilent Technologies). The same mutagenesis procedure was used to generate all *NAP1* mutants in this study. Mutated constructs were integrated into the HZX01 strain at the endogenous *NAP1* promoter region.

FRAP. FRAP analysis was performed using an inverted confocal laser LSM700 microscope (Carl Zeiss). The septin ring was bleached with a 488-nm laser for 25 iterations at 50% intensity. After the bleaching, images were collected every 1 min. Fluorescence intensity was analyzed using ImageJ. For each strain at each cell cycle stage examined, five individual recovery curves were determined. Average values of the bleached region of the septin ring were calculated. A reference cell in the imaging field was used to correct for general bleaching. The statistical analysis and the graphs were done using Prism software.

Virulence assays. *C. albicans* cells were grown overnight at 30°C in yeast extract-peptone-dextrose (YPD). Cells were washed twice in phosphate-buffered saline (PBS) and diluted with PBS to 5×10^6 cells/ml. Two hundred microliters of the cell suspension was injected into each BALB/c mouse. For each strain, 12 mice were injected. Two mice were sacrificed 5 h and 2 days postinjection for quantifying CFU/kidney. Kidneys were homogenized individually with a mortar and pestle for 1 min, and then serial dilutions of the homogenate were plated onto YPD plates for growth at 30°C for 2 days before the colonies were counted. The remaining 8 mice were monitored for 20 days, and a mouse was considered to be dead when it had lost 20% of its body weight or become moribund. The statistical analysis and the graphs were done using Prism software. Animal experiments were carried out according to National Advisory Committee for Laboratory Animal research guidelines, and all procedures were approved by the IACUC of the Agency for Science, Technology and Research of Singapore.

RNA isolation. Total RNA was isolated from log-phase yeast cells in YPD using the RNeasy minikit from Qiagen. Per extraction, ~2×10^7 cells were used, and cells were disrupted with a MicroSmash MS-100 beater (Tomy Medico, Tokyo, Japan).

Microarray analysis. Arrays were purchased from Microarrays Inc. (Huntsville, AL) and processed according to the manufacturer's instructions and published protocols (45, 46). Arrays were scanned using the GenePix 4000B Axon Instruments scanner (Molecular Devices, CA). Images were analyzed using the GenePix Pro 6.0 software (Molecular Devices). Microarray data were analyzed using the limma package (version 3.14.4) from the R/Bioconductor collection (43). Briefly, background intensity was corrected using the "normexp" method. Probes with a background-corrected intensity of >50 in both channels were removed from further analysis. Arrays were then normalized using print tip loess normalization, and differential expression was assessed using an empirical Bayes moderated *t* test. Tests were controlled for multiple testing using a Benjamini and Hochberg false discovery rate (45). Where multiple probes for a single gene were significant at a 5% FDR, fold change was calculated as the mean of significant probes.

SUPPLEMENTAL MATERIAL

Supplemental material for this article may be found at http://mbio.asm.org/lookup/suppl/doi:10.1128/mBio.00915-13/-/DCSupplemental.

Figure S1, EPS file, 0.4 MB.
Figure S2, EPS file, 0.3 MB.
Figure S3, EPS file, 2 MB.
Table S1, DOC file, 0.1 MB.
Table S2, XLS file, 0.1 MB.
Table S3, DOCX file, 0.1 MB.

ACKNOWLEDGMENTS

This study was supported by the Agency for Science, Technology and Research, Singapore.

We thank Jaime Correa-Bordes and Peter Sudbery for providing strains and Peter Sudbery and members of the Wang lab for critically reading the manuscript.

REFERENCES

1. **Hartwell LH.** 1971. Genetic control of the cell division cycle in yeast. IV. Genes controlling bud emergence and cytokinesis. Exp. Cell Res. **69:** 265–276. http://dx.doi.org/10.1016/0014-4827(71)90223-0.
2. **Oh Y, Bi E.** 2011. Septin structure and function in yeast and beyond. Trends Cell Biol. **21:**141–148. http://dx.doi.org/10.1016/j.tcb.2010.11.006.
3. **Saarikangas J, Barral Y.** 2011. The emerging functions of septins in metazoans. EMBO Rep. **12:**1118–1126. http://dx.doi.org/10.1038/embor.2011.193.
4. **Spiliotis ET, Gladfelter AS.** 2012. Spatial guidance of cell asymmetry: septin GTPases show the way. Traffic **13:**195–203. http://dx.doi.org/10.1111/j.1600-0854.2011.01268.x.
5. **Bertin A, McMurray MA, Grob P, Park SS, Garcia G III, Patanwala I, Ng HL, Alber T, Thorner J, Nogales E.** 2008. Saccharomyces cerevisiae septins: supramolecular organization of heterooligomers and the mechanism of filament assembly. Proc. Natl. Acad. Sci. U. S. A. **105:**8274–8279. http://dx.doi.org/10.1073/pnas.0803330105.
6. **Longtine MS, Theesfeld CL, McMillan JN, Weaver E, Pringle JR, Lew DJ.** 2000. Septin-dependent assembly of a cell cycle-regulatory module in Saccharomyces cerevisiae. Mol. Cell. Biol. **20:**4049–4061. http://dx.doi.org/10.1128/MCB.20.11.4049-4061.2000.
7. **Warenda AJ, Konopka JB.** 2002. Septin function in *Candida albicans* morphogenesis. Mol. Biol. Cell **13:**2732–2746. http://dx.doi.org/10.1091/mbc.E02-01-0013.
8. **Keaton MA, Lew DJ.** 2006. Eavesdropping on the cytoskeleton: progress and controversy in the yeast morphogenesis checkpoint. Curr. Opin. Microbiol. **9:**540–546. http://dx.doi.org/10.1016/j.mib.2006.10.004.
9. **Smolka MB, Chen SH, Maddox PS, Enserink JM, Albuquerque CP, Wei XX, Desai A, Kolodner RD, Zhou H.** 2006. An FHA domain-mediated protein interaction network of Rad53 reveals its role in polarized cell growth. J. Cell Biol. **175:**743–753. http://dx.doi.org/10.1083/jcb.200605081.
10. **Castillon GA, Adames NR, Rosello CH, Seidel HS, Longtine MS, Cooper JA, Heil-Chapdelaine RA.** 2003. Septins have a dual role in controlling mitotic exit in budding yeast. Curr. Biol. **13:**654–658. http://dx.doi.org/10.1016/S0960-9822(03)00247-1.
11. **Barral Y, Mermall V, Mooseker MS, Snyder M.** 2000. Compartmentalization of the cell cortex by septins is required for maintenance of cell polarity in yeast. Mol. Cell **5:**841–851. http://dx.doi.org/10.1016/S1097-2765(00)80324-X.
12. **Takizawa PA, DeRisi JL, Wilhelm JE, Vale RD.** 2000. Plasma membrane compartmentalization in yeast by messenger RNA transport and a septin diffusion barrier. Science **290:**341–344. http://dx.doi.org/10.1126/science.290.5490.341.
13. **Li CR, Lee RT, Wang YM, Zheng XD, Wang Y.** 2007. *Candida albicans* hyphal morphogenesis occurs in Sec3p-independent and Sec3p-dependent phases separated by septin ring formation. J. Cell Sci. **120:** 1898–1907. http://dx.doi.org/10.1242/jcs.002931.
14. **Gladfelter AS, Pringle JR, Lew DJ.** 2001. The septin cortex at the yeast mother-bud neck. Curr. Opin. Microbiol. **4:**681–689. http://dx.doi.org/10.1016/S1369-5274(01)00269-7.
15. **McMurray MA, Thorner J.** 2009. Septins: molecular partitioning and the generation of cellular asymmetry. Cell Div. **4:**18. http://dx.doi.org/10.1186/1747-1028-4-18.
16. **Gladfelter AS, Zyla TR, Lew DJ.** 2004. Genetic interactions among regulators of septin organization. Eukaryot. Cell **3:**847–854. http://dx.doi.org/10.1128/EC.3.4.847-854.2004.
17. **Tjandra H, Compton J, Kellogg D.** 1998. Control of mitotic events by the Cdc42 GTPase, the Clb2 cyclin and a member of the PAK kinase family. Curr. Biol. **8:**991–1000. http://dx.doi.org/10.1016/S0960-9822(07)00419-8.
18. **Altman R, Kellogg D.** 1997. Control of mitotic events by Nap1 and the Gin4 kinase. J. Cell Biol. **138:**119–130. http://dx.doi.org/10.1083/jcb.138.1.119.
19. **Li CR, Yong JY, Wang YM, Wang Y.** 2012. CDK regulates septin organization through cell-cycle-dependent phosphorylation of the Nim1-related kinase Gin4. J. Cell Sci. **125:**2533–2543. http://dx.doi.org/10.1242/jcs.104497.
20. **Sinha I, Wang YM, Philp R, Li CR, Yap WH, Wang Y.** 2007. Cyclin-dependent kinases control septin phosphorylation in *Candida albicans* hyphal development. Dev. Cell **13:**421–432. http://dx.doi.org/10.1016/j.devcel.2007.06.011.
21. **Ishimi Y, Yasuda H, Hirosumi J, Hanaoka F, Yamada M.** 1983. A protein which facilitates assembly of nucleosome-like structures in vitro in mammalian cells. J. Biochem. **94:**735–744.
22. **Zlatanova J, Seebart C, Tomschik M.** 2007. Nap1: taking a closer look at

a juggler protein of extraordinary skills. FASEB J. **21:**1294–1310. http://dx.doi.org/10.1096/fj.06-7199rev.
23. **Kellogg DR, Murray AW.** 1995. NAP1 acts with Clb1 to perform mitotic functions and to suppress polar bud growth in budding yeast. J. Cell Biol. **130:**675–685. http://dx.doi.org/10.1083/jcb.130.3.675.
24. **Ohkuni K, Shirahige K, Kikuchi A.** 2003. Genome-wide expression analysis of NAP1 in Saccharomyces cerevisiae. Biochem. Biophys. Res. Commun. **306:**5–9. http://dx.doi.org/10.1016/S0006-291X(03)00907-0.
25. **Miyaji-Yamaguchi M, Kato K, Nakano R, Akashi T, Kikuchi A, Nagata K.** 2003. Involvement of nucleocytoplasmic shuttling of yeast Nap1 in mitotic progression. Mol. Cell. Biol. **23:**6672–6684. http://dx.doi.org/10.1128/MCB.23.18.6672-6684.2003.
26. **Park YJ, Luger K.** 2006. The structure of nucleosome assembly protein 1. Proc. Natl. Acad. Sci. U. S. A. **103:**1248–1253. http://dx.doi.org/10.1073/pnas.0508002103.
27. **Calvert ME, Keck KM, Ptak C, Shabanowitz J, Hunt DF, Pemberton LF.** 2008. Phosphorylation by casein kinase 2 regulates Nap1 localization and function. Mol. Cell. Biol. **28:**1313–1325. http://dx.doi.org/10.1128/MCB.01035-07.
28. **Corner BE, Magee PT.** 1997. *Candida* pathogenesis: unravelling the threads of infection. Curr. Biol. **7:**R691–R694. http://dx.doi.org/10.1016/S0960-9822(06)00357-5.
29. **Jacobsen ID, Wilson D, Wächtler B, Brunke S, Naglik JR, Hube B.** 2012. *Candida albicans* dimorphism as a therapeutic target. Expert Rev. Anti Infect. Ther. **10:**85–93. http://dx.doi.org/10.1586/eri.11.152.
30. **Sudbery PE.** 2001. The germ tubes of *Candida albicans* hyphae and pseudohyphae show different patterns of septin ring localization. Mol. Microbiol. **41:**19–31. http://dx.doi.org/10.1046/j.1365-2958.2001.02459.x.
31. **Warenda AJ, Kauffman S, Sherrill TP, Becker JM, Konopka JB.** 2003. *Candida albicans* septin mutants are defective for invasive growth and virulence. Infect. Immun. **71:**4045–4051. http://dx.doi.org/10.1128/IAI.71.7.4045-4051.2003.
32. **Zheng X, Wang Y, Wang Y.** 2004. Hgc1, a novel hypha-specific G1 cyclin-related protein regulates *Candida albicans* hyphal morphogenesis. EMBO J. **23:**1845–1856. http://dx.doi.org/10.1038/sj.emboj.7600195.
33. **Berman J.** 2006. Morphogenesis and cell cycle progression in *Candida albicans*. Curr. Opin. Microbiol. **9:**595–601. http://dx.doi.org/10.1016/j.mib.2006.10.007.
34. **Sudbery PE.** 2011. Growth of *Candida albicans* hyphae. Nat. Rev. Microbiol. **9:**737–748. http://dx.doi.org/10.1038/nrmicro2636.
35. **Longtine MS, DeMarini DJ, Valencik ML, Al-Awar OS, Fares H, De Virgilio C, Pringle JR.** 1996. The septins: roles in cytokinesis and other processes. Curr. Opin. Cell Biol. **8:**106–119. http://dx.doi.org/10.1016/S0955-0674(96)80054-8.
36. **Kinoshita E, Kinoshita-Kikuta E, Takiyama K, Koike T.** 2006. Phosphate-binding tag, a new tool to visualize phosphorylated proteins. Mol. Cell. Proteomics **5:**749–757.
37. **Dobbelaere J, Gentry MS, Hallberg RL, Barral Y.** 2003. Phosphorylation-dependent regulation of septin dynamics during the cell cycle. Dev. Cell **4:**345–357. http://dx.doi.org/10.1016/S1534-5807(03)00061-3.
38. **Clemente-Blanco A, González-Novo A, Machín F, Caballero-Lima D, Aragón L, Sánchez M, de Aldana CR, Jiménez J, Correa-Bordes J.** 2006. The Cdc14p phosphatase affects late cell-cycle events and morphogenesis in *Candida albicans*. J. Cell Sci. **119:**1130–1143. http://dx.doi.org/10.1242/jcs.02820.
39. **Wightman R, Bates S, Amornrrattanapan P, Sudbery P.** 2004. In *Candida albicans*, the Nim1 kinases Gin4 and Hsl1 negatively regulate pseudohypha formation and Gin4 also controls septin organization. J. Cell Biol. **164:**581–591. http://dx.doi.org/10.1083/jcb.200307176.
40. **Lew DJ.** 2003. The morphogenesis checkpoint: how yeast cells watch their figures. Curr. Opin. Cell Biol. **15:**648–653. http://dx.doi.org/10.1016/j.ceb.2003.09.001.
41. **Umeyama T, Kaneko A, Nagai Y, Hanaoka N, Tanabe K, Takano Y, Niimi M, Uehara Y.** 2005. *Candida albicans* protein kinase CaHsl1p regulates cell elongation and virulence. Mol. Microbiol. **55:**381–395. http://dx.doi.org/10.1111/j.1365-2958.2004.04405.x.
42. **González-Novo A, Correa-Bordes J, Labrador L, Sánchez M, Vázquez de Aldana CR, Jiménez J.** 2008. Sep7 is essential to modify septin ring dynamics and inhibit cell separation during *Candida albicans* hyphal growth. Mol. Biol. Cell **19:**1509–1518. http://dx.doi.org/10.1091/mbc.E07-09-0876.
43. **Mitchell L, Lau A, Lambert JP, Zhou H, Fong Y, Couture JF, Figeys D, Baetz K.** 2011. Regulation of septin dynamics by the *Saccharomyces cerevisiae* lysine acetyltransferase NuA4. PLoS One **6:**e25336. http://dx.doi.org/10.1371/journal.pone.0025336.
44. **Murad AM, Lee PR, Broadbent ID, Barelle CJ, Brown AJ.** 2000. CIp10, an efficient and convenient integrating vector for *Candida albicans*. Yeast **16:**325–327. http://dx.doi.org/10.1002/1097-0061(20000315)16:4.
45. **Bennett RJ, Uhl MA, Miller MG, Johnson AD.** 2003. Identification and characterization of a *Candida albicans* mating pheromone. Mol. Cell. Biol. **23:**8189–8201. http://dx.doi.org/10.1128/MCB.23.22.8189-8201.2003.
46. **Kruppa MD.** 2009. *Candida albicans* gene expression in an in vivo infection model. Methods Mol. Biol. **499:**77–83. http://dx.doi.org/10.1007/978-1-60327-151-6_9.
47. **Wilson RB, Davis D, Enloe BM, Mitchell AP.** 2000. A recyclable *Candida albicans URA3* cassette for PCR product-directed gene disruptions. Yeast **16:**65–70. http://dx.doi.org/10.1002/(SICI)1097-0061(20000115)16:1.